

Morphological Versatility in the Self-Assembly of Val-Ala and Ala-Val Dipeptides

Hakan Erdogan,[†] Esra Babur,[†] Mehmet Yilmaz,[†] Elif Candas,[‡] Merve Gordesel,[§] Yavuz Dede,[§] Ersin Emre Oren,[‡] Gokcen Birlik Demirel,^{||} Mustafa Kemal Ozturk,[⊥] Mustafa Selman Yavuz,[#] and Gokhan Demirel^{*,†}

[†]Bio-inspired Materials Research Laboratory (BIMREL), Department of Chemistry, Gazi University, 06500 Ankara, Turkey

[‡]Bionanodesign Laboratory, Department of Biomedical Engineering, TOBB University of Economics and Technology, 06560 Ankara, Turkey

[§]Theoretical/Computational Chemistry Research Laboratory, Department of Chemistry, Gazi University, 06900 Ankara, Turkey

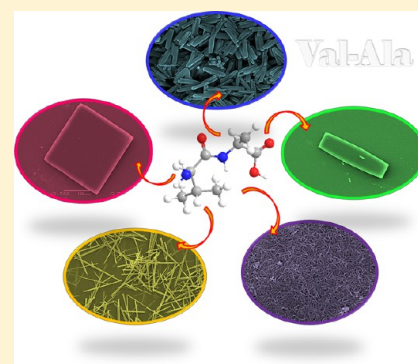
^{||}Department of Chemistry, Gazi University, Polatlı, 06500 Ankara, Turkey

[⊥]Department of Physics, Gazi University, 06500 Ankara, Turkey

[#]Department of Metallurgy and Materials Engineering, Selcuk University, 42075 Konya, Turkey

Supporting Information

ABSTRACT: Since the discovery of dipeptide self-assembly, diphenylalanine (Phe-Phe)-based dipeptides have been widely investigated in a variety of fields. Although various supramolecular Phe-Phe-based structures including tubes, vesicles, fibrils, sheets, necklaces, flakes, ribbons, and wires have been demonstrated by manipulating the external physical or chemical conditions applied, studies of the morphological diversity of dipeptides other than Phe-Phe are still required to understand both how these small molecules respond to external conditions such as the type of solvent and how the peptide sequence affects self-assembly and the corresponding molecular structures. In this work, we investigated the self-assembly of valine-alanine (Val-Ala) and alanine-valine (Ala-Val) dipeptides by varying the solvent medium. It was observed that Val-Ala dipeptide molecules may generate unique self-assembly-based morphologies in response to the solvent medium used. Interestingly, when Ala-Val dipeptides were utilized as a peptide source instead of Val-Ala, we observed distinct differences in the final dipeptide structures. We believe that such manipulation may not only provide us with a better understanding of the fundamentals of the dipeptide self-assembly process but also may enable us to generate novel peptide-based materials for various applications.



1. INTRODUCTION

Molecular self-assembly is a natural process in which molecules spontaneously and reversibly form ordered aggregates through a number of attractive and repulsive forces.^{1–4} In nature, many important biological structures including the DNA double helix, proteins, and cell membranes are formed through a self-assembly process by balancing covalent and noncovalent interactions. These processes not only play a crucial role in nature but also provide a powerful and simple strategy for developing bionanomaterials with unique properties.^{5–8} Over the past few decades, a number of biological molecules including peptides, proteins, DNAs, and lipids have been successfully utilized to create such functional materials due to their capacity for specific molecular recognition and simple modification, their biocompatibility, and their availability.^{8–10} Since the pioneering work by Reches and Gazit,¹¹ the dipeptide diphenylalanine (Phe-Phe), among all biological building blocks, has been considered one of the simplest biological molecules that can self-assemble into ordered structures. In

2012, Gazit and co-workers reported that phenylalanine molecules also self-assemble into amyloid-like fibrillar structures at high concentration.¹² Although various supramolecular Phe-Phe-based structures including tubes,¹¹ vesicles,¹³ fibrils,¹⁴ plates,¹⁵ flakes,⁴ necklaces,¹⁶ ribbons,¹⁷ and wires¹⁸ have been demonstrated by manipulating the external conditions^{19,20} or by adding small molecules such as Congo red, the morphological diversity of dipeptides other than Phe-Phe has largely been unexplored.

Experimental and modeling studies toward the understanding of peptide self-assembly are in their infancy, and accurate force field parameters required to model the peptide–peptide and peptide–solvent interactions are still under development. The diverse range of peptides and solvents that need to be characterized further confounds the solution to this

Received: May 20, 2014

Revised: June 9, 2015

Published: June 18, 2015

problem.^{21,22} Thus, the fabrication of new peptide structures with the desired properties is mainly explored by trial and error studies. Recently, Frederix et al. reported a computational analysis for all possible tripeptide sequence ($20^3 = 8000$) to identify peptide building blocks that could form well-ordered nanostructures in a water medium.²³ According to their complete aggregation-propensity (AP) analysis, they found that tripeptides having a higher AP score contain a pair of adjacent aromatic amino acids and at least one phenylalanine residue. In their computational analysis, however, they have used a limited selection criterion, mainly based on hydrophilicity, and they conducted studies only in a water medium for tripeptides. Recently, it has been demonstrated that the self-assembly of peptides may be manipulated by changing the solvent medium or introducing organic/inorganic molecules during their assembly process.^{18–20} In addition, peptides lacking aromatic moieties may also assemble into ordered structures.²⁴ Although computational efforts combined with simple experimental validations represent an important milestone in the development of peptide sequences with predicted self-assembly behavior, comprehending the full potential of the self-assembly of peptides regarding the molecular structure, sequence, and solvent medium is still a major challenge.

In the literature, the first example of a dipeptide-based nanostructure was reported by Gorbitz and Gunderson using a valine-alanine (Val-Ala) dipeptide.²⁴ Val-Ala dipeptides can self-assemble into ordered nanostructures through spiral head-to-tail hydrogen bonding. Although the crystalline framework of Val-Ala structures is held together by hydrogen bonding, the inner walls of nanochannels generated by the hydrocarbon fragments of Val-Ala are mainly hydrophobic. Inspired by these unique features of Val-Ala, Comotti et al. proposed that Val-Ala-based porous nanostructures can be effectively utilized for the absorption of environmentally and energetically relevant gases such as carbon dioxide, methane, and hydrogen.²⁵ Apart from the application of Val-Ala-based structures for the absorption, separation, and storage of the gas molecules, there have been only a few studies related to understanding the self-assembly mechanism of these structures and the possibility of controlling their final morphologies by adjusting the external conditions, which is necessary in evaluating the potential applications of Val-Ala as an organic framework material.

In this work, the self-assembly of Val-Ala dipeptides was evaluated in various solvent media. We also performed the same experiments by using alanine-valine (Ala-Val) dipeptides, which are the reverse analogous of the Val-Ala dipeptide. We found that Val-Ala dipeptide molecules generate various self-assembled micro-/nanostructures such as square plates, wires, rectangular plates, networks, and rods depending on the solvent or solvent mixture used, whereas Ala-Val dipeptides did not self-assemble into any distinct ordered structure under the same conditions. Such manipulations not only provide us with a better understanding of the fundamentals of the molecular self-assembly of these dipeptides but also make them attractive building blocks for the design of novel peptide-based materials of various shapes.

2. EXPERIMENTAL SECTION

2.1. Self-Assembly of Dipeptides. Unless otherwise stated, lyophilized Val-Ala and Ala-Val dipeptides (Bachem AG, Switzerland) were dissolved in pyridine, 2-propanol, ethanol, acetone, methanol, toluene, hexane, acetonitrile, or chloroform at a concentration of 2.0 mg/mL at 50 °C for 5 min and cooled to room temperature. To avoid

any preaggregation, fresh solutions were prepared for each experiment. Each peptide solution (50 μ L) was then placed on cleaned silicon wafers or glass slides and dried until the solvent evaporated.

To explore the solubility of Val-Ala and Ala-Val, solvents that were used in our work were first weighed into a beaker with the use of an analytical balance. Excess dipeptide (Val-Ala or Ala-Val) was then added to the beaker and placed in a shaker at room temperature. After 2 h, the beaker was removed and filtered through Whatman grade 1 filter paper and dried in an oven at 45 °C. The amount of solute in the filtrate was determined by the complete evaporation of solvent.

2.2. Characterization. All peptide morphologies were characterized by a JEOL JSM-6060 scanning electron microscope (SEM) at an acceleration voltage of 10 kV after the samples were coated with a thin layer of gold. A Fourier transform infrared (FTIR) spectrometer (Thermo Nicolet IR) operated in attenuated total reflection mode was used to collect IR spectra of the dipeptide samples. The spectra were recorded with a 4 cm^{-1} resolution. X-ray diffraction (XRD) measurements were obtained using Rigaku Ultima-IV X-ray diffractometer. The diffracted intensity of Cu $K\alpha$ radiation (40 kV and 30 mA) was measured at a scan rate of 2°/min over 2θ values ranging from 2.5 to 75°. For Raman experiments, a Delta Nu Examiner Raman microscopy system equipped with a 785 nm laser source, a motorized microscope stage sample holder, and a cooled charge-coupled device (CCD) detector was used over the wavenumber range of 200–2000 cm^{-1} . The instrument parameters were as follows: 20 \times objective, 3 μm spot size, 30 s acquisition time, and 150 mW laser power; baseline correction was performed for all measurements.

2.3. Molecular Modeling Studies. The molecular structures of Val-Ala and Ala-Val dipeptides were modeled using HyperChem's molecular modeling software (Hyperchem 7.5, USA). First, we built the linear forms of the peptides.²⁶ Then, the energy minimization of these peptides was carried out under implicit water solvation conditions using the conformational search module that finds the minimum-energy structures. To perform energy minimization, the module changes predefined dihedral angles randomly to create new initial structures. In each round of energy minimization, unique low-energy conformations are stored, and high-energy and duplicate structures are discarded. Using the conformational search module, we found 2500 different local minima on the potential energy surface using the CHARMM 27 force field,²⁷ and we chose the local minimum having the lowest energy as the global minimum or the lowest-energy conformation.^{26,28} The final lowest-energy conformations were visualized using VMD (Visual Molecular Dynamics) software.²⁹

Density functional theory (DFT)^{30–34} calculations were also performed by employing the (U)BLYP³⁵ functional in combination with the 6-31G(d,p)³⁶ basis set. No restrictions on symmetry were imposed. Vibrational frequency calculations using analytical second derivatives of energy were performed to ensure that the optimized structures correspond to true minima. Solvent molecules were loosely coordinated to various sites of the Val-Ala dipeptide and fully optimized. The interaction energies are those of the lowest-energy Val-Ala/solvent complexes obtained from various runs. All computations were performed with the Gaussian 09 suite of programs.³⁷

3. RESULTS AND DISCUSSION

First, we examined the solubilities of the dipeptide molecules in various solvents such as pyridine, 2-propanol, ethanol, acetone, methanol, toluene, hexane, acetonitrile, and chloroform media. The properties of the solvents, including their surface tension, dielectric constant, hydrogen bond donor (HBD),³⁸ and hydrogen bond acceptor (HBA)³⁹ abilities are presented in Table S1. To determine the solubilities of Val-Ala and Ala-Val in these solvents, we followed a simple approach based on gravimetric analysis. For Val-Ala, it was found that among the alcohols, methanol displays the highest solubility and dissolves more than 2.6 g/L of Val-Ala, whereas ethanol and 2-propanol dissolve 0.46 and 0.25 g/L of Val-Ala, respectively (Table S1). Moreover, hexane is a relatively poor solvent for Val-Ala, but

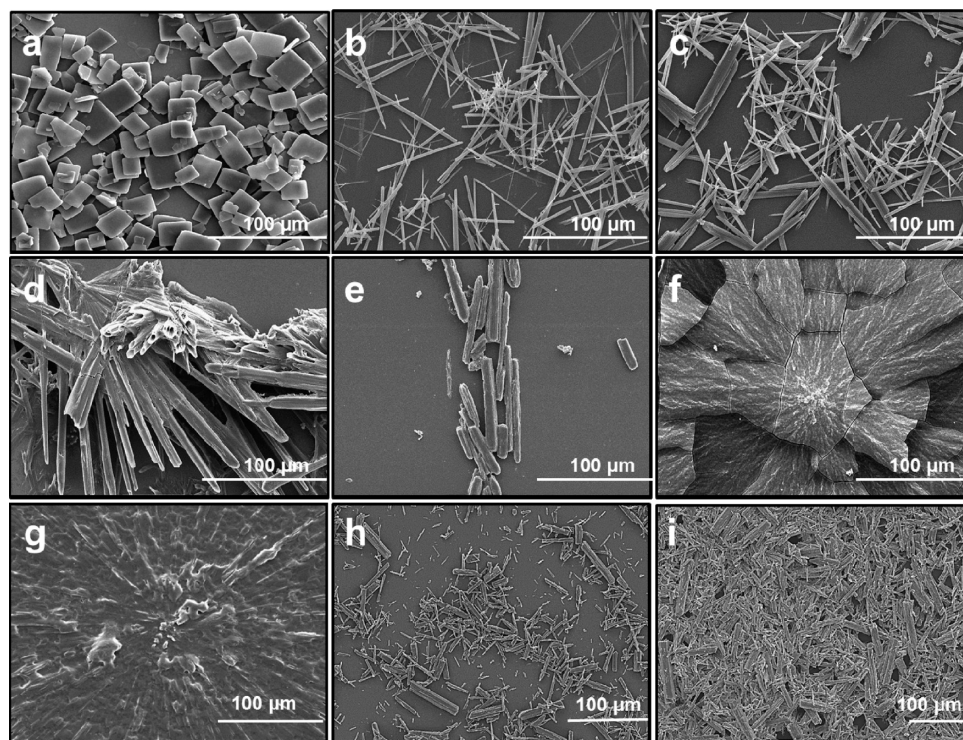


Figure 1. SEM images of Val-Ala structures in various solvent media: in (a) pyridine, (b) 2-propanol, (c) ethanol, (d) methanol, (e) acetone, (f) toluene, (g) hexane, (h) acetonitrile, and (i) chloroform.

toluene dissolves more than acetonitrile, acetone, and chloroform. Interestingly, pyridine exhibits a good ability to dissolve Val-Ala (~ 1.5 g/L). As for Ala-Val, similar solubility results were found for most of the solvents except for pyridine and 2-propanol (Table S1). Contrary to Val-Ala, 2-propanol dissolves Ala-Val more than 3-fold (~ 0.74 g/L), and pyridine dissolves Ala-Val less than about 4-fold as much as Val-Ala (~ 0.4 g/L). However, we should note that these solubility data are based on gravimetric analysis. Therefore, more precise experimental approaches are still necessary to extend the results of the solubility of Val-Ala and Ala-Val in different solvents.

The morphological and structural diversity of self-assembled dipeptide samples generated using different solvent media were then examined by SEM, XRD, and FTIR. SEM images reveal that Val-Ala formed highly dense, well-structured, and square-plate-like objects in pyridine (Figure 1a and Figure S1a). However, we could not observe any similar or ordered Val-Ala morphologies when structural analogues of pyridine were used as the solvent (i.e., aniline and pyrrole) (Figure S2). Interestingly, in the presence of 2-propanol, we observed that Val-Ala molecules generate a distinct wirelike structure, whereas in ethanol, the dipeptides formed irregular rodlike aggregates (Figure 1b). On the other hand, when acetone, methanol, hexane, acetonitrile, chloroform, and toluene were used as solvents, Val-Ala did not self-assemble into any ordered structure (Figure 1c–i).

The molecular basis of the observed morphological difference is first investigated by studying the interaction of solvent molecules with the Val-Ala dipeptides employing density functional theory (DFT).^{30–35} Val-Ala with the intramolecular ($-\text{NH}\cdots\text{HO}-$) H-bond possesses significant intermolecular H-bond donor (amine) and acceptor (carbonyl) sites. The interaction of different solvent molecules with these groups revealed that alcohols and water provide a stabilization larger

than 11 kcal mol^{-1} , which is approximately the interaction energy of two Val-Ala dipeptides (Table S2). On the other hand pyridine has a slightly lower interaction energy than Val-Ala/Val-Ala. Lying lower than pyridine, the Val-Ala/toluene interaction does not result in a large stabilization. Thus, we presumed that facile H-bonding might be an important factor in the formation of the less-ordered structures as the alcohols would generally tend to disrupt Val-Ala/Val-Ala interactions. In addition to these, Val-Ala/pyridine and Val-Ala/Val-Ala interactions are almost isoenergetic, and the slightly larger Val-Ala/Val-Ala interactions might be generating Val-Ala-based morphologies in the pyridine medium. Note the shape transition with the composition of the pyridine/2-propanol mixture (Figure 5).

We previously showed that the solvent medium, in which the self-assembly process of dipeptides occurs, plays a pivotal role in determining the final morphological diversity of the dipeptides.¹³ On the basis of our previous results¹³ and the quantum chemical calculations, suggesting the critical role of H-bonding, we hypothesized that the main driving force for the self-assembly of Val-Ala may be inter/intramolecular H-bonding interactions. Consistent with our hypothesis, Gorbitz reported that if a dipeptide molecule has comparatively small hydrophobic moieties in its structure, then three-dimensional intermolecular H-bonding interactions usually lead to a final structural motif.⁴⁰ According to Gorbitz's findings, Val-Ala molecules are arranged hexagonally through head-to-tail hydrogen bonding in which solvent molecules with a particularly strong ability to act as hydrogen-bonding donors tightly hold the peptide main chain together. The hydrogen bonds between the dipeptide and solvent can be formed mainly by the donation of hydrogen atoms of amino groups in each dipeptide to solvent molecules.²⁴ Pyridine is a hydrogen-bond acceptor solvent, and its HBA and HBD abilities are 0.64 and

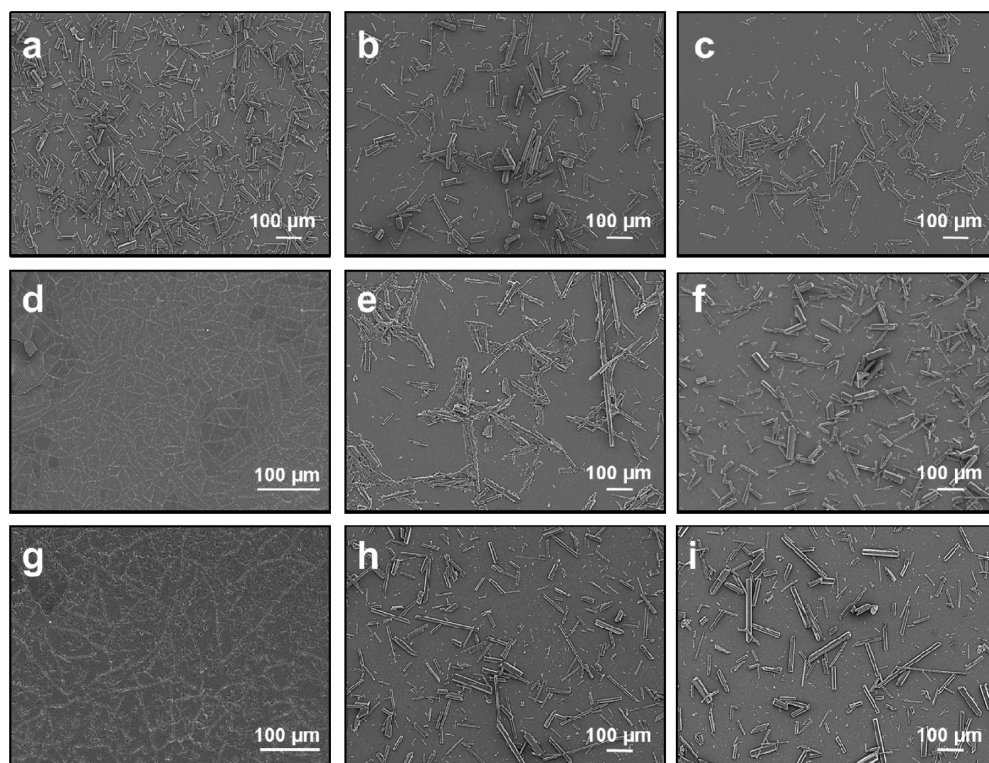


Figure 2. SEM images of Ala-Val structures in various solvent media: in (a) pyridine, (b) 2-propanol, (c) ethanol, (d) methanol, (e) acetone, (f) toluene, (g) hexane, (h) acetonitrile, and (i) chloroform.

0.00, respectively (Table S1). By contrast, the HBA and HBD values of 2-propanol are 0.95 and 0.76. In the case of 2-propanol, solvent molecules may interact with hydrogen atoms in amino groups of each peptide to form intermolecular hydrogen bonds. However, due to its high HBD ability and low surface tension, 2-propanol may also solvate the dipeptide molecules, preventing them from forming a more ordered structural morphology. In addition, we previously showed that solvents with a dielectric constant of more than 4 tend to solvate the hydrophilic headgroups of dipeptide molecules.¹³ In contrast, solvents with a dielectric constant of less than 4 lead to peptide molecules to form micelles, a network, or filmlike structures, thereby reducing the concentration of hydrophilic groups in the medium. The dielectric constant of 2-propanol is 18.3 at 25 °C; therefore, 2-propanol solvates the amino and carboxylate groups of Val-Ala. To minimize interfacial energy, Val-Ala molecules may be reordered and form wirelike morphologies in the 2-propanol solvent medium. Compared to 2-propanol, pyridine has different solvent properties which affect the self-assembly process of Val-Ala in different ways. The HBA ability of pyridine is 0.64; therefore, pyridine tends to form intermolecular H-bonds with dipeptide molecules. However, due to their lack of HBD ability and low dielectric constant (13.11 at 25 °C), pyridine molecules may not solvate Val-Ala molecules; therefore, Val-Ala dipeptide molecules or their extended sheet formations may interact with each other to form square-plate-like ordered morphologies. It should be noted that it is still not clear which solvent properties such as HBA ability, HBD ability, surface tension, and dielectric constant provide the main driving force in creating different dipeptide morphologies. We believe that each property, to some extent, contributes to the formation of the final morphology of the dipeptide structures.

The self-assembly of Val-Ala in pyridine and 2-propanol was also investigated using different dipeptide concentrations (0.5–4.0 mg/mL) (Figure S3). In the case of pyridine, irregular rodlike aggregates as well as platelike structures were observed at a concentration of 0.5 mg/mL. When the concentration was increased to 1.0 mg/mL, rectangular platelike Val-Ala structures were mainly identified. Unique square-plate-like structures were formed at a concentration of 2.0 mg/mL, whereas irregular plates were observed at a higher concentration (4.0 mg/mL) of dipeptide solution. On the other hand, unlike those in pyridine, Val-Ala dipeptides mainly formed irregular rodlike structures in 2-propanol at Val-Ala concentrations of 0.5, 1.0, and 4.0 mg/mL (Figure S3). However, at 2.0 mg/mL Val-Ala in 2-propanol, wirelike Val-Ala structures were observed.

We also explored the effect of solvent types on the self-assembly of Ala-Val dipeptides which are reverse analogous of Val-Ala. Interestingly, when Ala-Val dipeptides were used as the peptide source instead of Val-Ala, we observed distinct differences in the final dipeptide structures (Figure 2 and Figure S4). In the solvent media used, the Ala-Val dipeptides mainly generated irregular rodlike or film structures. In particular, rodlike Ala-Val structures were obtained in both pyridine and 2-propanol, whereas square-plate-like and wirelike Val-Ala structures were formed under the same conditions. The differences observed between the Val-Ala and Ala-Val dipeptides may be attributed to the positional disorder of methyl group side chains in L-Val residues within the Ala-Val structures.⁴¹ It has been reported that there is a shift from the favorable gauche[−]/trans side-chain conformation of L-Val in Ala-Val to the gauche⁺/gauche[−] conformation.⁴⁰ In addition, Ala-Val and Val-Ala dipeptides are structurally different in terms of their torsion angles. The experimental torsion angles for Val-Ala and Ala-Val are given in Table S3. Although the

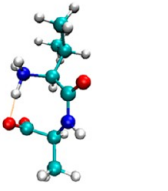
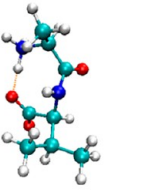
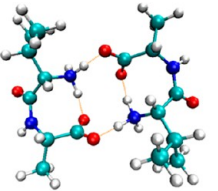
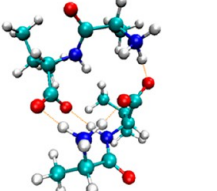
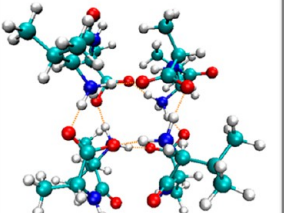
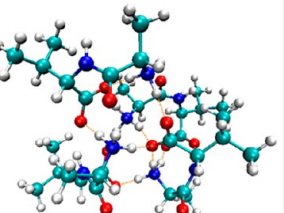
	Val-Ala	Ala-Val
Single mer	 # of intramer H-bonds: 1 # of intermer H-bonds: 0	 # of intramer H-bonds: 1 # of intermer H-bonds: 0
2-mer	 # of intramer H-bonds: 2 # of intermer H-bonds: 2	 # of intramer H-bonds: 1 # of intermer H-bonds: 3
4-mer	 # of intramer H-bonds: 2 # of intermer H-bonds: 8	 # of intramer H-bonds: 2 # of intermer H-bonds: 9

Figure 3. Hydrogen bond distributions and symmetries for single-, two-, and four-mer states of Val-Ala and Ala-Val dipeptides.

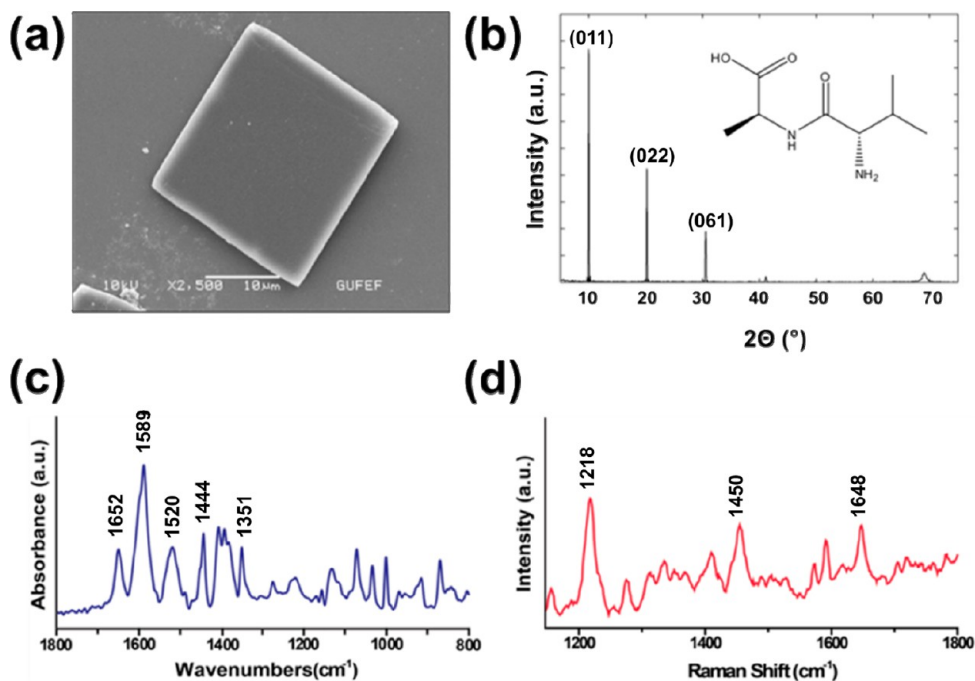


Figure 4. (a) SEM image, (b) XRD pattern, (c) FT-IR spectrum, and (d) Raman spectrum of square-plate-like Val-Ala morphology. The inset in (b) indicates the chemical structure of Val-Ala.

torsion angle of the peptide bond (ω_1) for both dipeptides has almost the same value (176.0° for Val-Ala and 175.98° for Ala-Val), other torsion angles (Ψ , ϕ , and χ) show significant differences. The Ψ_1 , ϕ_2 , Ψ_T , $\chi_1^{1,1}$, and $\chi_1^{1,2}$ values for Val-Ala are 162.9 , -150.6 , -28.2 , 53.6 , and -71.5° , in which these values for Ala-Val are 151.01 , -130.56 , -45.24 , -65.79 ($\chi_2^{1,1}$), and 171.72° ($\chi_2^{1,2}$), respectively.^{24,42} Because of these structural differences, the interactions between the Ala-Val dipeptides and

solvent molecules could be different from those observed for the Val-Ala dipeptides and therefore lead to the formation of different dipeptide structures.

The experiments clearly indicate that the self-assembly of dipeptides is a very complex process and is a function of both the peptide itself and the solvent type. Here, we also observed that the self-assembly depends on not only the amino acid content of the dipeptides but also the sequential arrangement

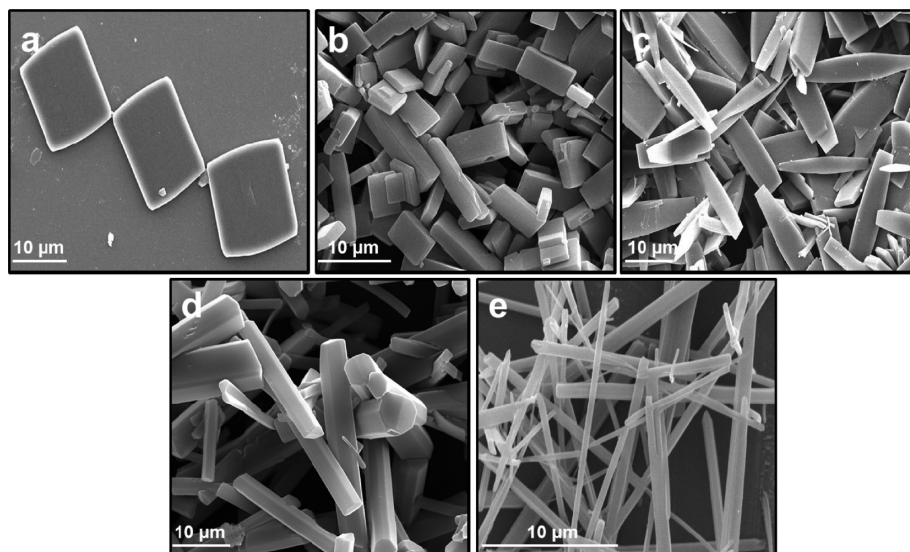


Figure 5. SEM images of Val-Ala generated at different pyridine/2-propanol ratios: (a) 0, (b) 30, (c) 50, (d) 70, and (e) 100% 2-propanol.

of the amino acid residues in a peptide.²² To shed some light on the self-assembly of these two dipeptides, we predicted the molecular structures of both Val-Ala and Ala-Val dipeptides with molecular dynamics studies employing the CHARMM 27 force field. Both peptides have a single H-bond between their N and C termini. This information is very limited to understanding the peptide–peptide interactions. Therefore, we calculated the 2- and 4-mer structures for both peptides. Figure 3 shows these H-bond distributions and the symmetries for these two types of dipeptides. Interestingly, when we compare the lowest-energy conformations of Val-Ala and Ala-Val dipeptides, we observed that the Val-Ala peptides have a higher tendency to have ordered structures. As we discussed previously, the interpeptide interactions are mainly governed by the hydrogen bonding, and the molecular conformations show that both peptides have four H-bonds in their 2-mer states. However, when we look for the nature of the H bonds, we observed that the Val-Ala dipeptides have two intra- and two interpeptide hydrogen bonds; on the other hand Ala-Val dipeptides have one intra- and three interpeptide hydrogen bonds. In the 4-mer case, we do have a similar tendency, and the Val-Ala dipeptides have a symmetrical distribution of the intra- and interpeptide hydrogen bonds, two and eight respectively, and the Ala-Val dipeptides have two intra- and nine interpeptide bonds. This symmetrical H-bond distribution may be the key for the observed long-range-ordered structures for Val-Ala peptides, which is not the case for Ala-Val peptides.

Among all of the dipeptide morphologies, the square-plate-like Val-Ala structures are unique and very interesting (Figure 4a). Therefore, to examine the molecular packing in this self-assembled system, X-ray diffraction analysis was performed. Figure 4b shows the XRD pattern of the square-plate-like Val-Ala structures. At wide angles ($2\theta = 5\text{--}75^\circ$), the XRD pattern reveals numerous sharp diffraction peaks, indicating extremely ordered molecular packing in this unique system. Three main sharp diffraction peaks appeared at $2\theta = 10.6, 20.8,$ and 31.1° , which correspond to the (011), (022), and (061) planes, respectively. Lattice parameters of $a = 20.71 \text{ \AA}$ and $c = 10.03 \text{ \AA}$ were calculated for these structures. The crystal size of the unit cell and the cell volume were calculated to be 761 nm and 3725.3 \AA^3 , respectively. The space group of the unit cell was

also found to be $P6_1$. Furthermore, the secondary structure of the square-plate-like Val-Ala assembly was investigated by FT-IR and Raman spectroscopy. Figure 4c shows the FT-IR spectra of the relevant Val-Ala structure. The amide I vibration, absorbing near 1650 cm^{-1} , arises mainly from the stretching vibration of $\text{C}=\text{O}$ bonds with minor contributions from the out-of-phase stretching vibration of $\text{C}-\text{N}$ bonds, deformation of $\text{C}-\text{C}-\text{N}$ bonds, and in-plane bending of $\text{N}-\text{H}$ bonds.⁴³ The bands at ~ 1590 and 1520 cm^{-1} indicate the bending vibration peaks of amide II. The band at approximately 1440 cm^{-1} indicates the vibration of polar groups in the Val-Ala structure. The square-plate-like peptide structures were also investigated by Raman spectroscopy (Figure 4d). The intense band at $\sim 1220 \text{ cm}^{-1}$ is assigned to the amide III band, indicating the β -sheet conformation of Val-Ala. The band at $\sim 1650 \text{ cm}^{-1}$ is another signature of the β -sheet-like conformation and can be distinguished easily from a similar amide I band produced by the α -helix-like conformation, which typically occurs at a wavenumber that is $\sim 10 \text{ cm}^{-1}$ lower. Bands between 1300 and 1500 cm^{-1} are also assigned to the bending of CH and CH_3 units and symmetric and asymmetric deformations of CH_3 in Val-Ala.^{44,45} On the basis of these data, it can be concluded that Val-Ala forms a β -sheet-like structure in the presence of pyridine due to strong intermolecular hydrogen-bonding interactions.

We also evaluated the Val-Ala assembly in various solvent mixtures with different volume ratios of pyridine/2-propanol, ethanol/acetone, ethanol/toluene, HFIP/pyridine, HFIP/2-propanol, HFIP/ethanol, and HFIP/acetone (Figures S5–S7). Although the presence of HFIP in the assembly medium led to a dramatic change in the resultant peptide morphologies, the Val-Ala assembly did not change to a great extent in the other solvent mixtures, except in the pyridine/2-propanol medium. Interestingly, when we mixed pyridine and 2-propanol in different proportions (0.7:0.3, 0.5:0.5, and 0.3:0.7 v/v), the dipeptides displayed a transition from a square-plate morphology to a wire morphology (Figure 5). As mentioned above, the Val-Ala dipeptide formed square-plate-like structures in pyridine and wire assemblies in 2-propanol. Mixing 30% 2-propanol with pyridine gave rise to a rectangular-plate-like Val-Ala morphology. In the system containing 50% 2-propanol, an

extended rectangular-plate morphology was observed. When the content of 2-propanol was increased to 70%, Val-Ala generated dense and well-structured rodlike objects. According to our results, the intermolecular hydrogen bonding of peptide main chains drives the formation of Val-Ala assemblies with a square-plate-like morphology in pyridine. Compared to pyridine, 2-propanol has a higher polarity and is considered to be a hydrogen bond donor. The addition of 2-propanol to pyridine increases the polarity of the solvents and enhances the solvent–peptide interactions.^{46,47}

Moreover, we investigated the changes in the crystal structure of Val-Ala with 2-propanol concentration. We observed a distinct change in the crystal structure of Val-Ala when the 2-propanol concentration in the self-assembly medium was increased (Figure 6). In 100% pyridine, three

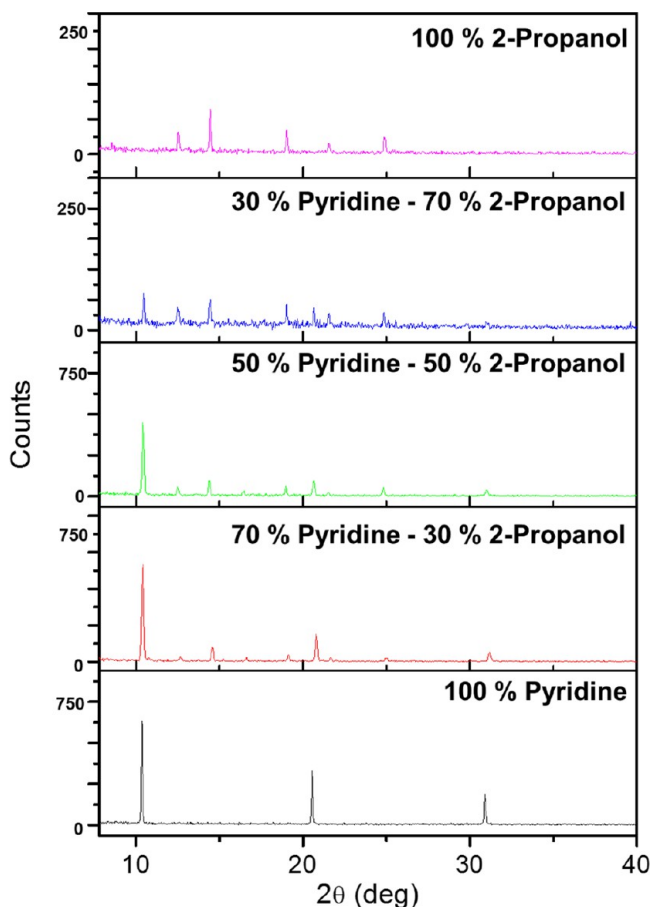


Figure 6. Powder XRD patterns of Val-Ala generated at different pyridine/2-propanol ratios.

main sharp diffraction peaks appeared at $2\theta = 10.6$, 20.8 , and 31.1° which correspond to the (011), (022), and (061) planes, respectively. The intensities of these diffraction peaks gradually decreased and finally disappeared in the presence of 100% 2-propanol. Furthermore, new diffraction peaks appeared at $2\theta = 12.5$, 14.5 , 19.1 , 21.5 , and 24.9° upon the addition of 2-propanol to the self-assembly medium, which also correspond to the (110), (020), (012), (031), and (130) planes, respectively. Consistent with the SEM images that we captured, the crystal structure of Val-Ala also changed depending on the concentration of 2-propanol in the self-assembly medium. The changes in crystal morphologies may be based on a change in

the relative surface energies of the growth facets. It is well known that the evolution of crystal morphology is mainly governed by continuously decreasing the total surface energy to reach a minimum point under a given condition.^{48,49} In this context, the final crystal shape can be identified on the basis of the surface energies of facets in the crystal structure by the Wulff construction. According to the Gibbs–Wulff theorem, the solvents, which preferentially adsorb onto a certain facet, would alter the order of surface energies during crystal growth.⁴⁹ Therefore, the selective adsorption results in decreasing the surface energy of the corresponding bound facet and hindering the crystal growth along their normal directions.⁴⁹ Because of the different solvent properties of pyridine and 2-propanol, solvent–dipeptide interactions along different orientations of the dipeptide crystal would change the surface stability of facets in terms of surface energy and hence the growth rates to the crystal surfaces.⁵⁰ However, the mechanism of this interesting process requires further investigation.

4. CONCLUSIONS

We demonstrated that Val-Ala dipeptides generate a wide range of structural morphologies in various solvent media. Highly ordered and crystalline unique square-plate-like Val-Ala structures can be formed in pure pyridine. We also observed clear structural differences in the same solvent media, when Ala-Val dipeptide molecules were used instead of Val-Ala. Quantum mechanical calculations hinted at the decisive role of Val-Ala/Val-Ala and Val-Ala/solvent H-bonding interactions in the morphological alterations. Molecular modeling studies also revealed that each one of the 2- and 4-mers of Val-Ala peptides have equally distributed intra- and intermolecular H-bonds; however, this is not the case for Ala-Val peptides. This structural difference may be the reason for the formation of long-range-ordered structures for Val-Ala dipeptides contrary to Ala-Val dipeptides. Our results suggest that the final morphology of the dipeptides is dictated, in part, by the properties of the solvent medium. However, it is still not clear which solvent properties, such as the HBA ability, HBD ability, surface tension, or dielectric constant, provide the main driving force in creating different dipeptide morphologies. We believe that the presented results may open the door to new opportunities for understanding and manipulating the organized patterns formed by dipeptide molecules. In addition, Val-Ala-based dipeptide structures with varying morphologies might offer new possibilities in creating biobased organic frameworks and in their applications, including CO_2 capture and H_2 gas storage.

■ ASSOCIATED CONTENT

Supporting Information

Property parameters of the solvents, solubilities of Val-Ala and Ala-Val in given solvents, high-magnification SEM images of the Val-Ala and Ala-Val dipeptide structures, SEM images of the Val-Ala dipeptides at varying concentrations, predicted molecular conformations of the Val-Ala and Ala-Val dipeptides, and additional characterization. The Supporting Information is available free of charge on the ACS Publications website at DOI: 10.1021/acs.langmuir.5b01406.

■ AUTHOR INFORMATION

Corresponding Author

*E-mail: nanobiotechnology@gmail.com.

Notes

The authors declare no competing financial interest.

ACKNOWLEDGMENTS

This work was supported by TUBITAK (grant no. 111M237). G.D. and E.E.O. also acknowledge support from the Turkish Academy of Sciences Distinguished Young Scientist Award (TUBA-GEBIP).

REFERENCES

- (1) Whitesides, G. M.; Grzybowski, B. Self-Assembly at All Scales. *Science* **2002**, *295*, 2418–2421.
- (2) Hartgerink, J. D.; Beniash, E.; Stupp, S. I. Self-assembly and Mineralization of Peptide-Amphiphile Nanofibers. *Science* **2001**, *294*, 1684–1688.
- (3) Ozin, G. A.; Hou, K.; Lotsch, B. V.; Cademartiri, L.; Puzzo, D. P.; Scotognella, F.; Ghadimi, A.; Thomson, J. Nanofabrication by Self-Assembly. *Mater. Today* **2009**, *12*, 12–23.
- (4) Demirel, G.; Buyukserin, F. Surface-Induced Self-Assembly of Dipeptides onto Nanotextured Surfaces. *Langmuir* **2011**, *27*, 12533–12538.
- (5) Sanchez, C.; Arribart, H.; Madeleine, M.; Guille, G. Biomimetic and Bioinspiration as Tools for the Design of Innovative Materials and Systems. *Nat. Mater.* **2005**, *4*, 277–288.
- (6) Nie, H. Z.; Kumacheva, E. Patterning Surfaces with Functional Polymers. *Nat. Mater.* **2008**, *7*, 277–290.
- (7) Ajayaghosh, A.; Praveen, V. K.; Vijayakumar, C. Organogels as Scaffolds for Excitation Energy Transfer and Light Harvesting. *Chem. Soc. Rev.* **2008**, *37*, 109–122.
- (8) Zhang, S. Fabrication of Novel Biomaterials through Molecular Self-Assembly. *Nat. Biotechnol.* **2003**, *21*, 1171–1178.
- (9) Yan, X.; Zhu, P.; Li, J. Self-Assembly and Application of Diphenylalanine-Based Nanostructures. *Chem. Soc. Rev.* **2010**, *39*, 1877–1890.
- (10) Yan, X.; He, Q.; Wang, K.; Duan, L.; Cui, Y.; Li, J. Transition of Cationic Dipeptide Nanotubes into Vesicles and Oligonucleotide Delivery. *Angew. Chem.* **2007**, *119*, 2483–2486.
- (11) Reches, M.; Gazit, E. Casting Metal Nanowires within Discrete Self-Assembled Peptide Nanotubes. *Science* **2003**, *300*, 625–627.
- (12) Abramovich, L. A.; Vaks, L.; Carny, O.; Trudler, D.; Magno, A.; Cafilisch, A.; Frenkel, D.; Gazit, E. Phenylalanine Assembly into Toxic Fibrils Suggests Amyloid Etiology in Phenylketonuria. *Nat. Chem. Biol.* **2012**, *8*, 701–706.
- (13) Demirel, G.; Malvadkar, N.; Demirel, M. C. Control of Protein Adsorption onto Core-Shell Tubular and Vesicular Structures of Diphenylalanine/Parylene. *Langmuir* **2010**, *26*, 1460–1463.
- (14) Huang, R.; Qi, W.; Su, R.; Zhao, J.; He, Z. Solvent and Surface Controlled Self-Assembly of Diphenylalanine Peptide: From microtubes to nanofibers. *Soft Matter* **2011**, *7*, 6418–6421.
- (15) Su, Y.; Yan, X.; Wang, A.; Fei, J.; Cui, Y.; He, Q.; Li, J. A Peony-Flower-like Hierarchical Mesocrystal Formed by Diphenylalanine. *J. Mater. Chem.* **2010**, *20*, 6734–6740.
- (16) Yuran, S.; Razvag, Y.; Reches, M. Coassembly of Aromatic Dipeptides into Biomolecular Necklaces. *ACS Nano* **2012**, *6*, 9559–9566.
- (17) Han, T. H.; Park, J. S.; Oh, J. K.; Kim, S. O. Morphology Control of One-Dimensional Peptide Nanostructures. *J. Nanosci. Nanotechnol.* **2008**, *8*, 5547–5550.
- (18) Erdogan, H.; Sakalak, H.; Yavuz, M. S.; Demirel, G. Laser-Triggered Degelation Control of Gold Nanoparticle Embedded Peptide Organogels. *Langmuir* **2013**, *29*, 6975–6982.
- (19) Rissanou, A. N.; Georgilis, E.; Kasotakis, E.; Mitraki, A.; Harmandaris, E. Effect of Solvents on the Self-Assembly of Dialanine and Diphenylalanine Peptides. *J. Phys. Chem. B* **2013**, *117*, 3962–3975.
- (20) Mason, T. O.; Chirgadze, D. Y.; Levin, A.; Abramovich, L. A.; Gazit, E.; Knowles, T. P. J.; Buell, A. K. Expanding the Solvent Chemical Space for Self-Assembly of Dipeptide Nanostructures. *ACS Nano* **2014**, *8*, 1243–1253.
- (21) Gazit, E. Molecular Self-Assembly: Searching Sequence Space. *Nat. Chem.* **2015**, *7*, 14–15.
- (22) Oren, E. E.; Tamerler, C.; Sahin, D.; Hnilova, M.; Seker, U. O. S.; Sarikaya, M.; Samudrala, R. A novel knowledge-based approach to design inorganic-binding peptides. *Bioinformatics* **2007**, *23*, 2816–2822.
- (23) Frederix, P. W. J. M.; Scott, G. G.; Abul-Haija, Y. M.; Kalafatic, D.; Pappas, C. G.; Javid, N.; Hunt, N. T.; Ulijn, R. V.; Tuttle, T. Exploring the Sequence Space for (tri-)Peptide Self-Assembly to Design and Discover New Hydrogels. *Nat. Chem.* **2015**, *7*, 30–37.
- (24) Gorbitz, C. H.; Gundersen, E. L-Valyl-L-alanine. *Acta Crystallogr., C* **1996**, *52*, 1764–1767.
- (25) Comotti, A.; Bracco, S.; Distefano, G.; Sozzani, P. Methane, Carbon Dioxide and Hydrogen Storage in Nanoporous Dipeptide-Based Materials. *Chem. Commun.* **2009**, 284–286.
- (26) Oren, E. E.; Tamerler, C.; Sarikaya, M. Metal recognition of septapeptides via polypod molecular architecture. *Nano Lett.* **2005**, *5*, 415–419.
- (27) MacKerell, A. D.; Bashford, D.; Bellott, M.; Dunbrack, R. L.; Evanseck, J. D.; Field, M. J.; et al. All-atom empirical potential for molecular modeling and dynamics studies of proteins. *J. Phys. Chem. B* **1998**, *102*, 3586–3616.
- (28) Cubellis, M. V.; Cailleux, F.; Blundell, T. L.; Lovell, S. C. Properties of polyproline II, a secondary structure element implicated in protein-protein interactions. *Proteins: Struct., Funct., Bioinf.* **2005**, *58*, 880–892.
- (29) Humphrey, W.; Dalke, A.; Schulten, K. VMD: Visual molecular dynamics. *J. Mol. Graphics* **1996**, *14*, 33–38.
- (30) Becke, A. D. Density-functional thermochemistry. III. The role of exact exchange. *J. Chem. Phys.* **1993**, *98*, 5648–5652.
- (31) Becke, A. D. Density-functional exchange-energy approximation with correct asymptotic-behavior. *Phys. Rev. A* **1988**, *38*, 3098–3100.
- (32) Parr, R. G.; Yang, W. *Density Functional Theory of Atoms and Molecules*; Oxford University Press: New York, 1989.
- (33) Kohn, W.; Becke, A. D.; Parr, R. G. Density functional theory of electronic structure. *J. Phys. Chem.* **1996**, *100*, 12974–12980.
- (34) Lee, C. T.; Yang, W. T.; Parr, R. G. Development of the Colle-Salvetti correlation energy formula into a functional of the electron-density. *Phys. Rev. B* **1988**, *37*, 785–789.
- (35) Hertwig, R. H.; Koch, W. On the parameterization of the local correlation functional. What is Becke-3-YP? *Chem. Phys. Lett.* **1997**, *268*, 345–351.
- (36) Ditchfield, R.; Hehre, W. J.; Pople, J. A. Self-consistent molecular orbital methods IX. An extended Gaussian-type basis for molecular-orbital studies of organic molecules. *J. Chem. Phys.* **1971**, *54*, 724–728.
- (37) Frisch, M. J.; Trucks, G. W.; Schlegel, H. B.; Scuseria, G. E.; et al. *Gaussian 09*, Revision A.1; Gaussian, Inc.: Wallingford, CT, 2009.
- (38) Kamlet, M. J.; Taft, R. W. The Solvatochromic Comparison Method. 2. The alpha-Scale of Solvent Hydrogen-Bond Donor (HBD) Acidities. *J. Am. Chem. Soc.* **1976**, *98*, 2886–2894.
- (39) Kamlet, M. J.; Taft, R. W. The Solvatochromic Comparison Method. I. The beta-Scale of Solvent Hydrogen-Bond Acceptor (HBA) Basicities. *J. Am. Chem. Soc.* **1976**, *98*, 377–383.
- (40) Gorbitz, C. H. Nanotubes from Hydrophobic Dipeptides: Pore Size Regulation through Side Chain Substitution. *New J. Chem.* **2003**, *27*, 1789–1793.
- (41) Moudrakovski, I.; Soldatov, D. V.; Ripmeester, J. A.; Sears, D. N.; Kameson, C. J. Xe NMR Lineshapes in Channels of Peptide Molecular Crystals. *Proc. Natl. Acad. Sci. U.S.A.* **2004**, *101*, 17924–17929.
- (42) Gorbitz, C. H. An Exceptionally Stable Peptide Nanotube System with Flexible Pores. *Acta Crystallogr., B* **2002**, *58*, 849–854.
- (43) Barth, A.; Zscherp, C. What Vibrations Tell Us About Proteins. *Q. Rev. Biophys.* **2002**, *35*, 369–430.
- (44) Zheng, R.; Zheng, X.; Dong, J.; Carey, P. R. Proteins Can Convert to β -Sheet in Single Crystals. *Protein Sci.* **2004**, *13*, 1288–1294.

(45) McColl, I. H.; Blanch, E. W.; Gill, A. C.; Rhie, A. G. O.; Ritchie, M. A.; Hecht, L.; Nielsen, K.; Barron, L. D. A New Perspective on β -Sheet Structures Using Vibrational Raman Optical Activity: From Poly(L-lysine) to the Prion Protein. *J. Am. Chem. Soc.* **2003**, *125*, 10019–10026.

(46) Kar, S.; Wu, K. W.; Hsu, I. J.; Lee, C. R.; Tai, Y. Study of The Nano-Morphological Versatility by Self-Assembly of a Peptide Mimetic Molecule in Response To Physical and Chemical Stimuli. *Chem. Commun.* **2014**, *50*, 2638–2641.

(47) Su, Y.; He, Q.; Yan, X.; Fei, J.; Cui, Y.; Li, J. Peptide Mesocrystals as Templates to Create an Au Surface with Stronger Surface-Enhanced Raman Spectroscopic Properties. *Chem.—Eur. J.* **2011**, *17*, 3370–3375.

(48) Chen, W.; Kuang, Q.; Wang, Q.; Xie, Z. Engineering a High Energy Surface of Anatase TiO₂ Crystals Towards Enhanced Performance for Energy Conversion and Environmental Applications. *RSC Adv.* **2015**, *5*, 20396–20409.

(49) Liu, G.; Yu, J. C.; Lu, G. Q. M.; Cheng, H. M. Crystal Facet Engineering of Semiconductor Photocatalysts: Motivations, Advances and Unique Properties. *Chem. Commun.* **2011**, *47*, 6763–6783.

(50) Lovette, M. A.; Browning, A. R.; Griffin, D. W.; Sizemore, J. P.; Synder, R. C.; Doherty, M. F. Crystal Shape Engineering. *Ind. Eng. Chem. Res.* **2008**, *47*, 9812–9833.